5_2021_Hanif et al_Adv. Nat. Sci. Nanosci. Nanotechnol.

by Hanif Amrulloh

Submission date: 19-Dec-2021 11:37AM (UTC+0700)
Submission ID: 1733572439
File name: 5_2021_Hanif_et_al_Adv._Nat._Sci._Nanosci._Nanotechnol..pdf (1.61M)
Word count: 4763
Character count: 24861

IOP Publishing | Vietnam Academy of Science and Technology
Advances in Natural Sciences: Nanoscience and Nanotechnology
Adv. Nat. Sci.: Nanosci. Nanotechnol. 12 (2021) 015006 (8pp)
https://doi.org/10.1088/2043-6254/abde39

Bioactivities of nano-scale magnesium oxide prepared using aqueous extract of *Moringa Oleifera* leaves as green agent

Hanif Amrulloh[1], Awalul Fatiqin[2], Wasinton Simanjuntak[3], Hapin Afriyani[3] and Annissa Annissa[4]

[1] Department of Mathematics Education, Faculty of Tarbiya, Institute for Islamic Studies Ma'arif NU (IAIMNU) Metro Lampung, Indonesia
[2] Department of Biology, Faculty of Science and Technology, Islamic State University of Raden Fatah Palembang, Indonesia
[3] Department of Chemistry, Faculty of Mathematics and Natural Sciences, Lampung University, Indonesia
[4] Department of Public Health, Health Faculty, Faletehan University, Indonesia

E-mail: amrulloh.hanif@iaimnumetrolampung.ac.id

Received 30 June 2020
Accepted for publication 6 September 2020
Published 4 February 2021

Abstract

In this research, nano-size MgO (NS-MgO) was prepared from $MgCl_2$ solution using aqueous extract of *Moringa oleifera* leaves (AEMOL) as green agent. Preparation procedure involved mixing of $MgCl_2.6H_2O$ solution and the AEMOL, followed by dropwise addition of NaOH solution. The formation of NS-MgO in this synthesis was confirmed using UV-Vis absorption. The spherical crystal structure of NS-MgO was confirmed by XRD analysis. The average particle size of the synthesised NS-MgO was found between 40–70 nm using scanning electron microscopy (SEM) and transmission electron microscopy (TEM) images and particle size analyser (PSA) results. Based on the maximum inhibition concentration (MIC) it was found that the NS-MgO has good antibacterial activity against *S. aureus*, *E. faecalis*, *E. coli*, and *S. dysenteriae* bacteria (MIC values: 250–500 μg ml^{-1}), and much stronger antifungal activity against *A. flavus*, *A. niger*, and *C. albican* (MIC values: 62.5–125 μg ml^{-1}). These findings suggest prospective potential of NS-MgO synthesised as therapeutic candidate for the treatment of candidiasis.

Keywords: bioactivities, *M. oleifera*, nano-size MgO, antifungal, candidiasis
Classification numbers: 2.05, 4.02, 5.00, 5.08

1. Introduction

Nanoparticle, which refers to a material having the size in the range of 1−100 nm, is acknowledged as versatile material due to superior properties compared to its bulk material [1]. Nanomaterial is known to possess excellent physical, chemical, optical, and biological properties that can be manipulated or arranged. With these characteristic flexibilities, various applications of nanomaterial are well documented, such as engineering material [2], catalysis [3], pigment [4], environmental remediation agent [5] and pharmaceutical agent [6].

Among various nanomaterials that have been developed, nano-size MgO (NS-MgO) is of particular interest for its bioactivities as antifungal [7], antibacterial [8] and anticancer [9]. In recognising these useful applications, many attempts in synthesising NS-MgO have been made, involving chemical and physical methods such as precipitation [9], vapour chemical deposition [10], solvothermal [11], electrochemical [12–14], sonochemistry [15], microwave [16], and sol-gel [17]. While these methods are acknowledged to enable the production of NS-MgO, they are also hampered by drawbacks for being expensive or toxic to the environment. To alleviate some of the practical disadvantages associated with physical and chemical methods, one initiative that continues to gain interest is development of environmentally friendly technology, based on biological approaches [18, 19]. For NS-MgO,

several biosynthetic routes have been reported, such as the use of plant extracts [18], fungi [20], and bacteria [21]. Many reports on the use of plant extract are available in literatures, for example the use of *Bauhinia purpurea* leaf extract [19], leaf extract of *Amaranthus tricolor*, *Andrographis paniculata*, and *Amaranthus blitum, Mucuna pruriens* (L.) ore extract [21], and orange peel extract [22].

Another plant that has continuously attracted scientific interest is *Moringa oleifera* (*M. oleifera*) [23, 24]. This plant, which is known as the 'tree of life' in many cultures, is widely grown commercially in Africa and almost throughout Asia and Southeast Asia. In some areas, the immature wood will and the leaves are consumed since these parts of the plant are rich in nutrients [25]. Various products of *M. oleifera* can be used as an anti-inflammatory, antihypertensive, antidiabetic, hepatoprotection [26], natural agent to reduce microbial load in water treatment [27, 28] natural coagulant for removal of reactive dyes from water [28], and functional food [29]. Razis *et al* [25] reported the potential health benefits of *M. oleifera* for high content of antioxidant component and antimicrobial characteristics. In the field synthetic science, *M. oleifera* extract has been widely used to synthesise metal nanoparticles, metal compounds, and metal oxides. As an example, Sundrarajan *et al* [30] reported preparation of nano-size hydroxyapatite [$Ca_5(PO_4)_3(OH)_2$] using *M. oleifera* flower extract. In another study by Elumalai *et al* [31], *M. oleifera* leaf extract was applied to synthesise zinc oxide nanoparticles (ZnO NPs). The use of *M. oleifera* leaf extract has also been reported by Das *et al* [32] to synthesise bismuth nanoparticles. However, there is still limited information on the use of *M. oleifera* extract for synthesis of NS-MgO.

In recognition of successful application of plant extracts as green agent for synthesis of variety of materials, this research was conducted to study the use of aqueous extracts of *M. oleifera* leaves (AEMOL) for preparation of NS-MgO. This study was attempted since the use of aqueous extract of this particular plant for NS-MgO preparation is still limited. The NS-MgO prepared was then characterised using different techniques, and then tested for bioactivities as antioxidant, antibacterial and antifungal.

2. Materials and methods

2.1. Materials

Fresh *M. oleifera* leaves were collected from the plants that grow naturally around the City of Metro, Lampung, Indonesia during September 2019 (figure 1). Laboratory grade magnesium chloride hexahydrate ($MgCl_2.6H_2O$), Folin-Ciocalteu reagents, sodium carbonate (Na_2CO_3), resazurin, gallic acid, catechin, aluminum chloride ($AlCl_3$), sodium nitrite ($NaNO_2$), sodium hydroxide (NaOH) and nano-size MgO (NS-MgO) standard were purchased from Merck Sigma-Aldrich Reagent Pte, Singapore.

Figure 1. Photograph of *M. oleifera* leaves used in this study.

2.2. Experimental procedures

2.2.1. Preparation of AEMOL extract. Fresh *M. oleifera* leaves were washed using flowing water, and then dried under direct sunlight, and finally ground into powder and stored at room temperature. 4 g of *M. oleifera* leaf powder was soaked in 100 ml of distilled water and heated at 60 °C for 20 min until the powder was thoroughly mixed with the water. The mixture was left for 1 h, subsequently filtered using Whatman filter paper No. 1 to separate the AEMOL from the residue.

2.2.2. Phytochemicals analysis. The AEMOL extract *M. oleifera* was subjected to phytochemical analysis to detect the presence of carbohydrates, amino acids, glycosides, polyphenols, saponins, steroids, flavonoids, tannins, and alkaloids. Total phenolic was estimated using the Follin-Ciocalteu test [33], and the result was expressed as microgram per milligram ($\mu g\ mg^{-1}$) gallic acid equivalent (GAE). Total flavonoid content was determined by the colorimetric $AlCl_3$ method, using catechin as standard and expressed as microgram per milligram ($\mu g\ mg^{-1}$) equivalent of catechin (CE) [34].

2.2.3. Preparation of nano-size MgO (NS-MgO). To synthesise NS-MgO, an aqueous extract of 50 ml AEMOL was mixed with 50 ml $MgCl_2.6H_2O$ solution 1 mM in a beaker at 90 °C and stirred at 600 rpm. The solution of NaOH 1 M was added dropwise until the colour of the mixture faded out and precipitate was formed. The mixture was left for 3 h to maximise the synthesis process. To optimise NS-MgO synthesis, various factors such as $MgCl_2.6H_2O$ concentration (0.5–5 mM) and AEMOL dose (10%–70%) were evaluated by using UV-Vis spectroscopy. NS-MgO synthesised under optimal conditions was centrifuged at 7500 rpm at room temperature and re-dispersed in deionised water and methanol

Table 1. Phytochemicals analysis of AEMOL.

Chemical constituents	Testing methods	M. oleifera leaf aqueous extract
Alkaloids	Dragendroff's test	+
Flavonoids	Shinoda test	+
Saponins	Foam test	+
Carbohydrate	Anthrone test	+
Polyphenols	Puncal-D	+
Proteins	Ninhydrin test	+
Asam amino	Millon's test	+
Phenolics	Ferric chloride test	+
Triterpens	Salkowski test	−
Anthraquinones	Borntragges test	−

+ = presence; − = absence.

(99%) to remove biological residues. The process was repeated twice, and the solid was dried at 100 °C. The solid was subjected to calcination at 600 °C for 5 h to optimise the formation of NS-MgO.

2.2.4. Characterisations of NS-MgO. Several techniques were used to characterise the NS-MgO prepared. The formation of NS-MgO was indicated by the change in the colour of the reaction mixture during the progress of the reaction and recorded with UV-Vis spectroscopy (Analytic Jena Specord 200 Plus) by scanning the sample in the wavelength range of 200–800 nm. The morphology of the NS-MgO was studied with scanning electron microscopy (SEM, FEI Inspect-S50) and transmission electron microscopy (TEM, Jeol Jem 1400) and the average particle size by the particle size analyser (PSA, Horiba SZ 100z). The crystal structure was confirmed by X-ray diffraction (XRD, PANAnalytical Expert Pro). Thermogravimetry analysis was carried out using thermal gravimetric analyser (TGA, Linseiss STA P 1600).

2.2.5. Bioactivity test

2.2.5.1. Antioxidant. Antioxidant activity of AEMOL and NS-MgO was evaluated through 2,2-diphenyl-1-picrylhydrazyl (DPPH) radical testing in accordance with the procedure described by Das *et al* [34], using ascorbic acid as reference. DPPH 0.1 mM solution was prepared by dissolving in ethanol. 1 mg of ascorbic acid was dissolved in 1 ml of methanol. Dilution was carried out to make a standard solution of ascorbic acid with different concentrations (50–500 $\mu g\ \mu l^{-1}$). For each tube containing a standard solution of ascorbic acid (200 μl), 1 ml of 0.1 mM DPPH solution was added and continued with the addition of 800 μl Tris-HCl 50 mM buffer (pH 7.4). The final volume is adjusted to 4 ml using ethanol. Stock solutions for AEMOL, synthesised NS-MgO and standard NS-MgO were prepared by dissolving 1 mg of each sample in 1 ml of a suitable solvent (AEMOL using methanol and NS-MgO using DMSO).

Different aliquots of stock solution (50−500 $\mu g\ \mu l^{-1}$) were added to separate tubes, and the final volume was adjusted to 2 ml using ethanol. A total of 1 ml of 0.1 mM DPPH solution and 800 μl Tris-HCl 50 mM buffer (pH 7.4) was added to each tube. The control was made by mixing 1 ml DPPH 0.1 mM, 800 μl Tris-HCl 50 mM buffer (pH 7.4), and 2 ml ethanol. Absorbance at 517 nm was recorded by UV-Vis spectrophotometer after incubation for 30 min at room temperature. The percentage of antioxidant activity (AA %) was calculated using the following equation:

$$(\text{AA}\%) = \frac{\text{control absorbance} - \text{sample absorbance}}{\text{control absorbance}} \times 100\%. \quad (1)$$

The mean and standard deviation (SD) were calculated based on triplicate measurement.

2.2.5.2. Antibacterial and antifungal. Microorganism and inoculum preparation: The antibacterial activity of AEMOL and NS-MgO was evaluated against both gram-positive (*S. aureus* and *E. faecalis*) and gram-negative (*E. coli* and *S. dysenteriae*) obtained from the microbiology laboratory of Airlangga University. The fungal cultures of *A. flavus*, *A. niger*, and *C. albican* were obtained from the microbiology laboratory of Airlangga University. Bacterial and fungal cultures for testing were cultivated on nutrient agar (NA) tilted by selecting a colony from the Mueller-Hinton agar plate (MHA) after 24 h.

For standardised populations, a single bacterial or fungal colony was selected and transferred using a sterilised loop to the Mueller-Hinton broth (MHB), followed by continuous shaking at 100 rpm at 37 °C overnight. For the test of antibacterial and antifungal activity, the optical density of bacterial or fungal suspense was maintained at the 0.5 McFarland standard by adding sterilised MHB. Thus, the inoculum consists of several bacteria or fungi around 10^6-10^7 CFU ml^{-1}.

Minimum inhibition concentration (MIC) determination: To determine minimum inhibition concentration, the resazurin microtiter assay was utilised. This method was chosen since it is considered as the most rapid and inexpensive way to screen several microorganism isolates at the same time, and provides satisfying results [32, 35, 36]. The resazurin solution was prepared by dissolving a 270 mg tablet of resazurin in 40 ml of sterile distilled water. The test was carried out in 96-well plates under aseptic conditions. A volume of 100 μl of sample containing 600 $\mu g\ ml^{-1}$ was transferred into the well of the plate. Afterwards, 50 μl of bacterial or fungal suspense was added to all other wells, and the tested sample was serially diluted. Subsequently, 10 μl of resazurin solution was added to each well. To prevent dehydration, the plates were wrapped with film and incubated at 37 °C for 24 h. The colour change was visually observed. A blue to pink colour change was considered indicating cell growth. MIC was recorded at the lowest concentration where a colour change occurred. Streptomycin (antibacterial) and ketoconazole (antifungal) (10 $\mu g/500\ \mu l$) served as a positive control,

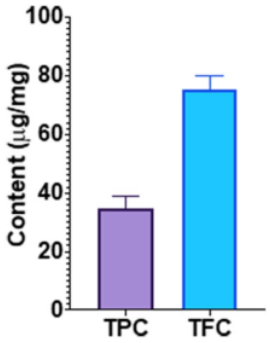

Figure 2. Total phenolic and flavonoid content of AEMOL. Notes: value is mean ± SD.

whereas a mixture of sterile distilled water and DMSO solvent with nutrient broth were used as negative controls.

3. Results and discussion

3.1. Chemical composition of plant extract

The qualitative evaluation of various biomolecules contained in AEMOL was carried out by different methods and the results are presented in table 1.

Table 1 shows that AEMOL contain biomolecules and fluorophore such as alkaloids, flavonoids, saponins, carbohydrates, polyphenols, proteins, amino acids and phenolics. The absence of triterpenes and anthraquinones is possible because they are not easily dissolved in water. A stabilising agent can be used as a precursor of nanoparticle synthesis (*in-situ* synthesis or one-pot synthesis) or can be added to nanoparticles that have been produced through chemical adsorption or grafting processes. Usually the stabiliser used is a large molecule/polymer that contains a functional group that can be chemically or physically adsorbed or bound to the surface of nanoparticles such as polysaccharides, polyvinyl alcohols, or polyacrylamides [37–39].

Total phenolic and flavonoid levels in AEMOL are 34.75 ± 4.03 (μg mg^{-1} GAE) and 74.28 ± 4.82 (μg mg^{-1} CE) respectively in dry powder, as shown in figure 2. The organic constituents of AEMOL are believed to play roles as reducing or chelating agents in the formation of NS-MgO. These roles are based on the reports by others on the successful use of aqueous extract of leaf [34], stem [40], fruit [41], peel [21, 22], and flower [23] for synthesis of NS-MgO.

3.2. Monitoring of NS-MgO formation

Formation of NS-MgO was monitored visually and using UV-Vis analysis. Visually, the process was observed through the change in the colour of the mixture from green to brown. The UV-Vis monitoring was carried out by measuring the absorbance around 290 nm as seen in figure 3. In previous studies [34], the formation of NS-MgO was indicated by the emergence of sharp peaks at about 270–290 nm.

To optimise the formation of NS-MgO synthesis, a reaction mixture containing 50% AEMOL with various concentrations of $MgCl_2.6H_2O$ (0.5–5 mM) was used and monitored using UV-Vis analysis (figure 3(c)). At a concentration of $MgCl_2.6H_2O$ 1 mM, the absorbance at maximum wavelength was found to reach the highest value, followed by decreasing values for the higher concentrations (2−5 mM) of $MgCl_2.6H_2O$ solution.

Other factors investigated are the reaction mixtures with different compositions (10%−70%) of AEMOL solution and 1 mM $MgCl_2.6H_2O$ solution, producing the UV-Vis spectra shown in figure 3(d). The results revealed that the maximum absorbance was observed for the sample with 50% AEMOL, and therefore the optimum conditions for the synthesis of NS-MgO in this study are the use of 1 mM of $MgCl_2.6H_2O$ solution with a 50% AEMOL.

3.3. NS-MgO characterisation

3.3.1. XRD. Crystal properties of dry NS-MgO were studied through XRD analysis. The pattern of XRD analysis is shown in figure 4. There are five diffraction peaks at 37.23; 42.92; 62.30; 74.73; and 78.63°, which correspond to the plane of MgO spherical crystal structure (JCPDS file 78-0430). According to the Debye-Scherrer equation [42], the average particle size was calculated to be 21 nm.

3.3.2. SEM and TEM. SEM and TEM images show that the shape of NS-MgO are spherical (figures 5(a)−(c)). SEM analysis data show that the synthesised NS-MgO is spherical with sizes ranging between 20 and 50 nm. Some larger nanoparticles are observed, which may be due to aggregation or overlap of particles. The size, shape, and morphology of the synthesised nanoparticles were confirmed by SEM and TEM imaging.

3.3.3. Particle size distribution analysis. To gain more insight regarding the particle size of the NS-MgO produced, the particle size distribution of the sample was determined using particle size analysis (PSA) technique. As displayed by the PSA result presented in figure 5(d), the particle sizes of the synthesised NS-MgO are in the range of 40 to 70 nm. With refers to general definition of nanomaterial as the material with the particle size in the range of 1–100 nm, the PSA result confirms the successful preparation of NS-MgO. Another interesting result with respect to the result of PSA is that the distribution of particles of the NS-MgO synthesised practically follows normal distribution pattern. In this regard, it can be observed that most of the particles have the size in the range of 50 to 55 nm.

3.3.4. Thermogravimetric analysis (TGA). To investigate thermal stability of the sample, the synthesised NS-MgO and the standard NS-MgO were subjected to TGA treatment, and the results are presented in figure 6. As can be seen in figure 6, for the standard NS-MgO, there is only one weight loss region, which is in the temperature range of 78 to 113 °C and resulted in 13.7% weight-loss. This weight loss is most

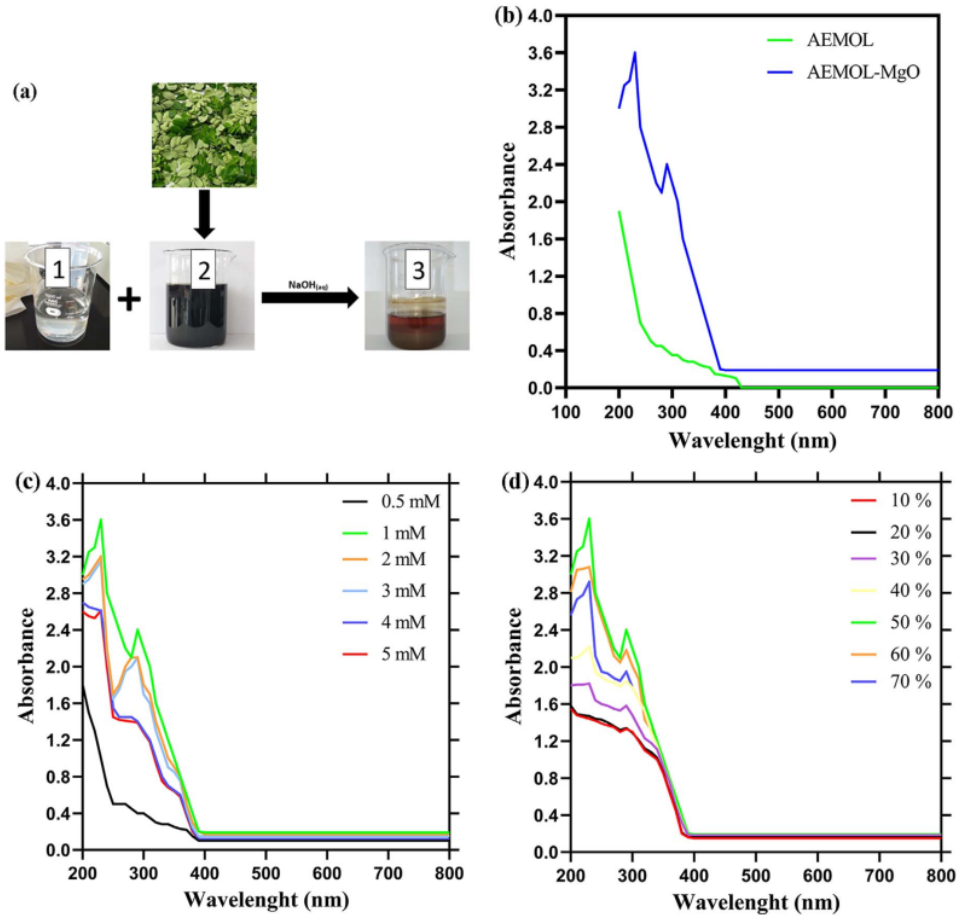

Figure 3. (a) Green synthesis of NS-MgO, (1) $MgCl_2.6H_2O$ solution, (2) AEMOL, (3) NS-MgO; (b) UV-Vis spectra of AEMOL and AEMOL containing MgO; (c) UV-Vis spectra of NS-MgO prepared at different $MgCl_2.6H_2O$ concentrations; (d) UV-Vis spectra of NS-MgO in AEMOL with different doses (%).

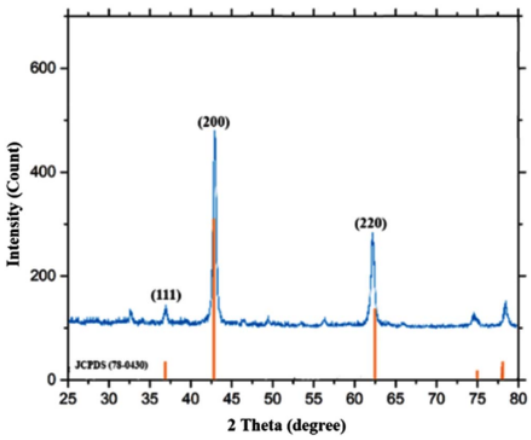

Figure 4. XRD pattern of the synthesised NS-MgO.

likely associated with the evaporation of adsorbed water by the samples. For the synthesised NS-MgO, gradual weight loss was observed, with the most significant losses of 19.75% in the region of 78 to 113 °C, and 40.15 % in the temperature range of 320 and 400 °C. This final loss is most likely due to thermal decomposition of residual organics contained in the AEMOL and trapped in the NS-MgO [43].

3.4. Bioactivity test

3.4.1. Antioxidant activity. In this study, antioxidant activity of AEMOL, synthesised NS-MgO, and standard NS-MgO was assessed by 2,2-diphenyl-1-picrylhydrazyl (DPPH) method using ascorbic acid as a positive control. This method, which is based on the free radical capture activity of DPPH, is often applied to study antioxidant activity of compounds present in medicinal plant extracts [44]. The experimental results, showing a general trend of increased

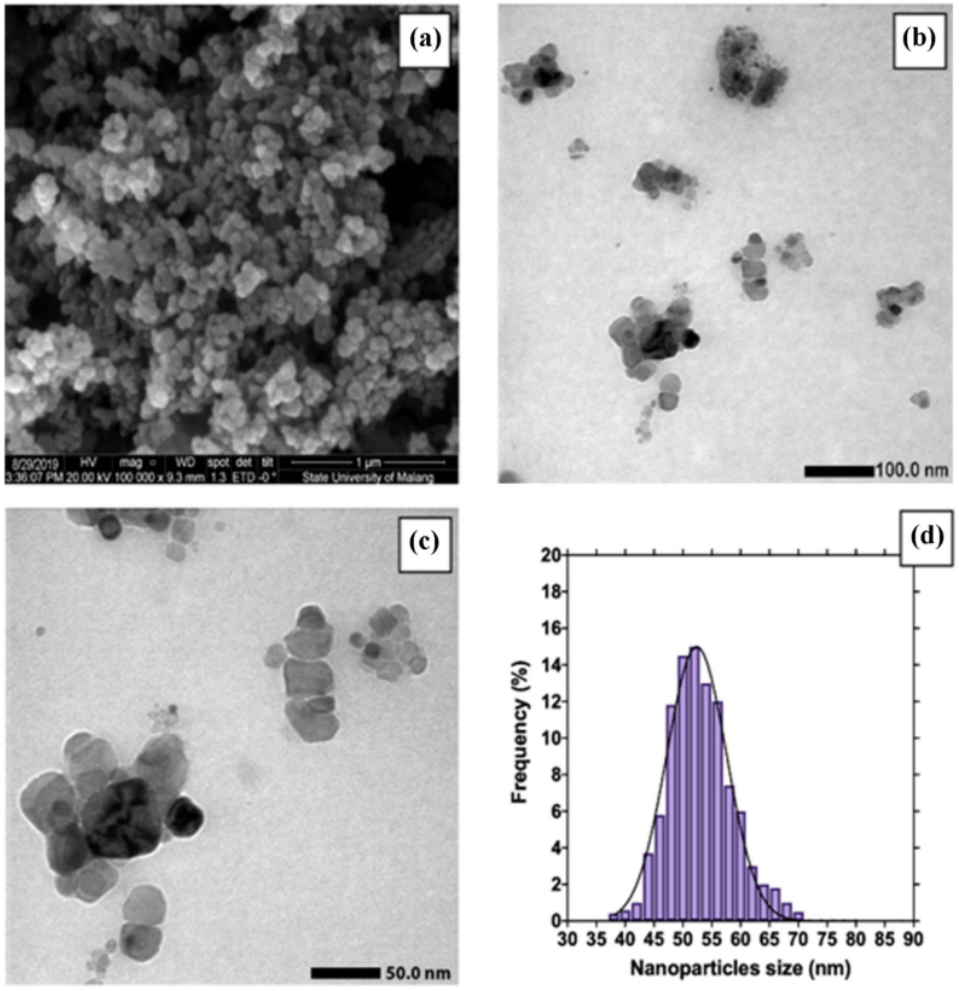

Figure 5. (a) SEM image of NS-MgO; (b) and (c) TEM images of NS-MgO at different magnifications; (d) particle size distribution.

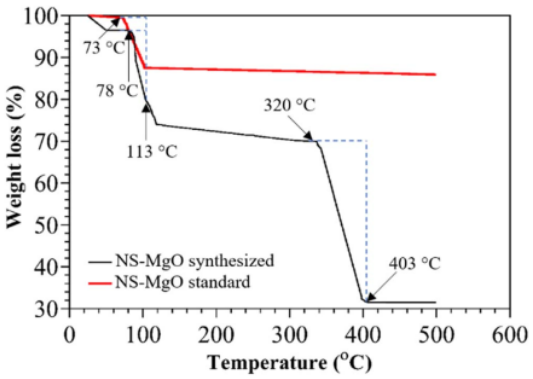

Figure 6. TGA profile of the calcined sample.

antioxidant activity of the samples as their concentrations increased, are presented in figure 7. The most interesting result is that the activity of the synthesised NS-MgO is very close to that of standard NS-MgO. This particular finding demonstrates that the method developed in this current study for NS-MgO synthesis is very promising for production of nanomaterials. It should also be mentioned that the results obtained in this study are in agreement with the results reported by others using nano-size ZnO [45], CuO [46], and MgO [34].

3.4.2. Antibacterial and antifungal activity. Antibacterial activity of AEMOL, synthesised NS-MgO and standard NS-MgO was evaluated against gram-positive bacteria (*S. aureus* and *E. faecalis*) and gram-negative bacteria (*E. coli* and *S. dysenteriae*) clinically isolated *in vitro*. The evaluation was

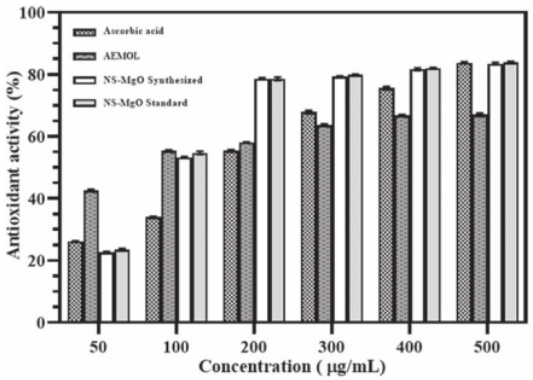

Figure 7. Antioxidant activity of AEMOL, synthesised NS-MgO and standard NS-MgO, using ascorbic acid as a positive control.

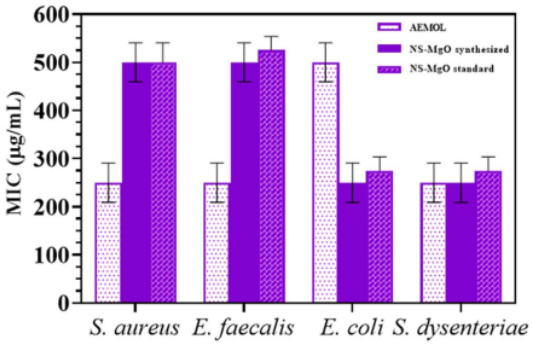

Figure 8. Antibacterial activity of AEMOL, synthesised NS-MgO and standard NS-MgO.

carried out using the method of resazurin microtiter assay plate, the antibacterial activities of the samples are compiled in figure 8.

As can be seen in figure 8, the MIC values of synthesised NS-MgO for the four bacteria are in the range of 250−500 μg ml^{-1}, and comparable to those observed for the standard NS-MgO (275−525 μg ml^{-1}). Compared to AEMOL, it can be seen that both NS-MgO samples have significantly higher MIC values against *S. aureus*; *E. faecalis,* lower values against *E. coli*, and comparable values against *S. dysenteriae*. In overall, it can be seen that the NS-MgO is more effective to combat *E. coli*, and *S. dysenteriae*, which are gram-negative bacteria, while for the gram-positive bacteria, their effectivities are lower than those of AEMOL. Different antibacterial activity against gram-positive and gram-negative bacteria is most likely related to the structure of the cell walls of the bacteria. Gram-positive bacteria have a thick layer of peptidoglycan without an outer membrane and contain teichoic acid. In contrast, gram-negative bacteria have a thin layer of peptidoglycan with an outer membrane that contains lipopolysaccharides. Because of this difference, each type of bacteria shows a different sensitivity [8].

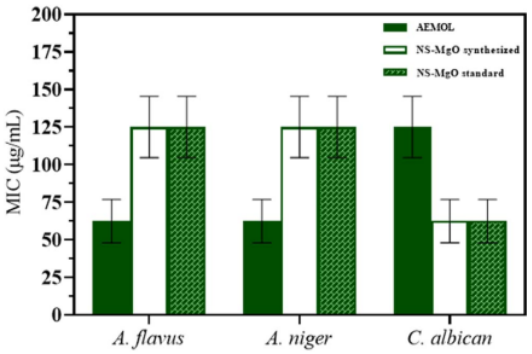

Figure 9. Antifungal activity of the samples against three types of fungi.

The method of resazurin microtiter assay plate was also applied to evaluate the antifungal activity of the samples against *A. flavus*, *A. niger*, and *C. albican*, as shown in figure 9.

As seen in figure 9, based on their MIC values, synthesised NS-MgO and standard NS-MgO exhibit comparable effectivity, with the MIC values against *A. flavus*, *A. niger,* and *C. albican* around 125, 125, and 62.5 μg ml^{-1}, while for the AEMOL, the MIC values are 62.5, 62.5 and 125 μg ml^{-1} respectively. Based on these MIC values it can be inferred that the NS-MgO samples have better activity against *C. albican*, compared to the AEMOL, but against *A. flavus*, and *A. niger*, the opposite is true. With respect to the bioactivities investigated, another important finding that should be noted is that the NS-MgO is more effective as antifungal rather than as antibacterial. These findings suggest that synthesised nano-scale MgO is promising as therapeutic candidate for the treatment of candidiasis.

4. Conclusions

The results of this study demonstrate that AEMOL is an effective green agent for synthesising NS-MgO. The formation of NS-MgO was confirmed by the information provided by various characterisation techniques applied. Characterisation using XRD technique confirms the existence of the NS-MgO as crystalline material, while the information regarding the particle size provided by SEM, TEM, and PSA suggests that the particle sizes are in the range of 40–70 nm. Bioactivity studies reveal that the antibacterial activity as well as antifungal activity of the NS-MgO synthesised is comparable to those of NS-MgO standard. Another important finding that should be noted is that the NS-MgO is more effective as antifungal agent, suggesting its prospective use for treatment of candidiasis.

Acknowledgments

This research supported by the Ministry of Religious Affairs Republic Indonesia through collaboration research BOPTN UIN Raden Fatah Palembang No: B-383/Un.09/PP.06/05/

2019. Furthermore, acknowledgment is also expressed for the full support from Laboratorium Sentral Mineral & Material Maju Universitas Negeri Malang, Direktorat Riset & Pengabdian Masyarakat Universitas Indonesia, and Laboratorium TEM Jurusan Kimia Universitas Gajah Mada for technical contributions in the research projects.

References

[1] Gmoshinski I V, Khotimchenko S A, Popov V O, Dzantiev B B, Zherdev A V, Demin V F and Buzulukov Y P 2013 *Russ. Chem. Rev.* **82** 48
[2] Seqqat R, Blaney L, Quesada D, Kumar B and Cumbal L 2019 *J. Nanotechnol.* **2019** 2850723
[3] Abdallah Y, Ogunyemi S O, Abdelazez A, Zhang M, Hong X, Ibrahim E, Hossain A, Fouad H, Li B and Chen J 2019 *BioMed. Res. Int.* **2019** 5620989
[4] Bilgili E, Hamey R and Scarlett B 2004 *China Particuology* **2** 93
[5] Kumari P, Alam M and Siddiqi W A 2019 *Sustain. Mater. Techno.* **22** e00128
[6] Luksiene Z 2017 *Food Preservation* ed A M Grumezescu (Cambridge: Academic) p 567
[7] La Rosa-García S C, Martínez-Torres P, Gómez-Cornelio S, Corral-Aguado M A, Quintana P and Gómez-Ortíz N M 2018 *J. Nanomater.* **2018** 3498527
[8] Nguyen N Y T, Grelling N, Wetteland C L, Rosario R and Liu H 2018 *Sci. Rep.* **8** 16260
[9] Camtakan Z, Erenturk S and Yusan S 2012 *Environ. Prog. Sustain. Energy* **31** 536
[10] Selvakumar N and Barshilia H C 2012 *Sol. Energy Mater. Sol. Cells* **98** 1
[11] Pilarska A A, Klapiszewski Ł and Jesionowski T 2017 *Powder Technol.* **319** 373
[12] Amrulloh H, Simanjuntak W and Situmeang R T M 2017 *ALKIMIA: Jurnal Ilmu Kimia dan Terapan* **1** 10
[13] Amrulloh H, Simanjuntak W, Situmeang R T M, Sagala S L, Bramawanto R, Fatiqin A, Nahrowi R and Zuniati M 2020 *Inorg. Nano-Met. Chem.* **50** 693
[14] Amrulloh H, Simanjuntak W, Situmeang R T M, Sagala S L, Bramawanto R and Nahrowi R 2019 *J. Pure App. Chem. Res.* **8** 87
[15] Štengl V, Bakardjieva S, Maříková M, Bezdička P and Šubrt J 2003 *Mater. Lett.* **57** 3998
[16] Makhluf S, Dror R, Nitzan Y, Abramovich Y, Jelinek R and Gedanken A 2005 *Adv. Funct. Mater.* **15** 1708
[17] Athar T, Hakeem A and Ahmed W 2012 *Adv. Sci. Lett.* **7** 27
[18] Jeevanandam J, Chan Y S and Danquah M K 2017 *New J. Chem.* **41** 2800
[19] Moodley J S, Krishna S B N, Pillay K, Sershen S and Govender P 2018 *Adv. Nat. Sci. Nanosci. Nanotech.* **9** 015011
[20] Raliya R, Tarafdar J C, Choudhary K, Mal P, Raturi A, Gautam R and Singh S K 2014 *J. Bionanosci.* **8** 34
[21] Mohanasrinivasan V, Subathra Devi C, Mehra A, Prakash S, Agarwal A, Selvarajan E and Jemimah Naine S 2018 *Bio. Nano Science* **8** 249
[22] Munjal S, Singh A and Kumar V 2017 *Int. J. Adv. Res. Chem. Sci.* **4** 36
[23] Abdallah E 2016 *Journal of Advances in Medical and Pharmaceutical Sciences* **5** 1
[24] Anand K, Tiloke C, Phulukdaree A, Ranjan B, Chuturgoon A, Singh S and Gengan R M 2016 *J. Photochem. Photobiol. B, Biol.* **165** 87
[25] Razis A F A, Ibrahim M D and Kntayya S B 2014 *Asian Pac. J. Cancer Prev.* **15** 8571
[26] Mbikay M 2012 *Front. Pharmacol.* **3** 24
[27] Bazrafshan E, Faridi H, Mostafapour F K and Mahvi A H 2013 *Asian J. Chem.* **25** 3557
[28] Jafari A and Mahvi A H 2015 *Environ. Eng. Manag. J.* **14** 2393
[29] Ma Z F, Ahmad J, Zhang H, Khan I and Muhammad S 2020 *S. Afr. J. Bot.* **129** 40
[30] Sundrarajan M, Jegatheeswaran S, Selvam S, Sanjeevi N and Balaji M 2015 *Mater. Des.* **88** 1183
[31] Elumalai K, Velmurugan S, Ravi S, Kathiravan V and Ashokkumar S 2015 *Spectrochim. Acta A Mol. Biomol. Spectrosc.* **143** 158
[32] Das P E, Majdalawieh A F, Abu-Yousef I A, Narasimhan S and Poltronieri P 2020 *Materials* **13** 876
[33] Magesh R, Poorani R M, Karthikeyan V, Sivakumar K and Mohanapriya C 2015 *Int. J. Pharmacogn. Phytochem. Res.* **7** 1066
[34] Das B, Moumita S, Ghosh S, Khan M I, Indira D, Jayabalan R, Tripathy S K, Mishra A and Balasubramanian P 2018 *Mater. Sci. Eng.* C **91** 436
[35] Monteiro M C *et al* 2012 *J. Biomol. Screen.* **17** 542
[36] Hudman D A and Sargentini N J 2013 *Springer Plus* **2** 55
[37] Thirumavalavan M, Huang K L and Lee J F 2013 *Colloids Surf. A Physicochem. Eng. Asp.* **417** 154
[38] Abdel-Aziz M S and Hezma A M 2013 *Polym. Plast. Technol. Eng.* **52** 1503
[39] Norazlina M S, Shanmugan S and Mutharasu D 2014 *Adv. Sci. Focus* **1** 362
[40] Gandhi R R, Senthil S, Rajappan R, Ramesh K, Gowri S, Suresh J and Sundrarajan M 2016 *J. Nanoeng. Nanomanuf.* **5** 70
[41] Ramanujam K and Sundrarajan M 2014 *J. Photochem. Photobiol. B, Biol.* **141** 296
[42] Nemade K R and Waghuley S A 2014 *Int. J. Met.* **2014** 389416
[43] Essien E R, Atasie V N, Oyebanji T O and Nwude D O 2020 *Chem. Pap.* **74** 2101
[44] Dewanjee S, Gangopadhyay M, Bhattacharya N, Khanra R and Dua T K 2015 *J. Pharm. Anal.* **5** 75
[45] Safawo T, Sandeep B V, Pola S and Tadesse A 2018 *Open Nano* **3** 56
[46] Dobrucka R 2018 *J. Inorg. Organomet. Polym. Mater.* **28** 812

5_2021_Hanif et al_Adv. Nat. Sci. Nanosci. Nanotechnol.

ORIGINALITY REPORT

17%	17%	7%	0%
SIMILARITY INDEX	INTERNET SOURCES	PUBLICATIONS	STUDENT PAPERS

PRIMARY SOURCES

1	www.mdpi.com Internet Source	6%
2	www.ajol.info Internet Source	6%
3	repository.lppm.unila.ac.id Internet Source	5%

Exclude quotes	On	Exclude matches	< 3%
Exclude bibliography	On		